

# Novel Design of a Self-Compensating Restrictor for Hydrostatic Bearings

Cho-Yu Yang\*, Wei-Chen Kao\*, Yi-Chen Wang\* and Cheng-Kuo Sung\*\*

**Keywords** : hydrostatic bearing, self-compensating restrictor; stiffness; load-carrying capacity.

## ABSTRACT

This paper proposes a design for a self-compensating restrictor for hydrostatic bearings. The proposed restrictor consists of a compensation block and two disc springs and offers the advantages of self-sensing compensation and easy installation. First, interrelated theories are presented on the self-compensating restrictor installed within the hydrostatic bearing. Second, equations are derived that govern the dimensionless relationship between the stiffness, gap, and resistance of the bearing land and the eternally applied load on the bearing. Influences of the design parameters on bearing performance and the feasibility of the design are then assessed both analytically and experimentally. The results of the theoretical analysis are then compared with the experimental results. These demonstrate that the proposed restrictor exhibits superior performance in terms of stiffness and load-carrying capacity. Furthermore, it has the advantage of simplicity in its manufacture and assembly.

## INTRODUCTION

The hydrostatic bearing was invented by Girard (1862). The hydrostatic bearing is composed of several bearing pads and associated flow restrictors and a bearing structure. In addition, auxiliary systems are required to maintain the operation of the bearing, which include an oil supply unit, an oil filter, and a cooling unit. The oil supply unit provides oil at high pressure that flows through the restrictors into the pockets of bearing pads to create high-pressure oil

films between the journal and the bearing. The hydrostatic bearing is therefore characterized by high stiffness and a large load-carrying capacity, and it experiences only a small friction force. These advantages have resulted in the hydrostatic bearing being widely employed in various types of precision machinery.

When a load is applied to the bearing, the pocket pressure, which varies in line with changes in the resistance of the restrictor and the gap in the bearing land, increases to bear the load. There are several types of flow restrictors, the bearing of which may differ in stiffness and load-carrying capacity. Fixed-type and pressure-sensing-type restrictors are primarily used in hydrostatic bearings. The capillary and orifice are fixed-type restrictors with constant flow resistance. Raimondi and Boyd (1957) constructed a theoretical model and developed analytical equations for bearings with capillary and orifice restrictors, respectively. The main type of pressure-sensing restrictor is the diaphragm, where flow resistance changes as pocket pressure varies. Mayer and Shaw (1963) found that a bearing with a pressure-sensing restrictor exhibited better stiffness. Conversely, Moshin (1962) found that a hydrostatic bearing with a diaphragm restrictor exhibited better static and dynamic stiffness than a bearing with a capillary or orifice restrictor under the same operating conditions. Tully (1977) proposed a hydrostatic bearing with extremely high stiffness over a substantial load range. This was achieved by optimally designing the configuration parameters of the diaphragm-type pressure-sensing restrictor.

In recent years, most research on pressure-sensing restrictors has focused on membrane-type restrictors (Phalle et al., 2011; Kotilainen, 2000; Kang et al., 2007), the designs of which are more complex than other fixed-type restrictors (Lai et al., 2017). Consequently, the design of these manufactured restrictors is often not as accurate. Membrane-type restrictors are therefore not widely used in hydrostatic bearings. The main parameters of membrane-type restrictors that are affected by accuracy are the structure size of the membrane, the gap in the membrane restrictor, and the stress area of the membrane (Gohara et al., 2014). It is therefore important to reduce the difficulty of manufacturing these parameters.

*Paper Received June, 2019. Revised September, 2019 Accepted October, 2019, Author for Correspondence: Cho-Yu Yang.*

*\* Graduate Student, Department of Power Mechanical Engineering, National Tsing Hua University, Taiwan 30013, ROC.*

*\*\* Associate Professor, Department of Power Mechanical Engineering, National Tsing Hua University, Taiwan 30013, ROC.*

This paper proposes a design for a self-compensating restrictor for hydrostatic bearings that produces a bearing with infinite stiffness and permits easy manufacturing and assembly. First, the configuration of the proposed self-compensating restrictor is introduced. The lumped parameter modeling method is then used to derive equations governing the dimensionless relationship between the load-carrying capacity, stiffness, and externally applied load. The influences of design parameters, such as the land length and pressure ratio, on bearing performance and the feasibility of the new design are explored both analytically and experimentally. Finally, the results of the theoretical analysis are compared with the experimental results.

### PHYSICAL MODEL AND GOVERNING EQUATION

Figure 1(a) shows the geometrical configuration of the proposed self-compensating restrictor to which a bearing is connected. The self-compensating restrictor consists of two disc springs and a compensation block. The compensation block is cylindrical in shape, with one circular flange. The disc springs are mounted on the top and bottom surfaces of the flange. When high-pressure oil flows into the restrictor, a gap in the self-compensating restrictor is formed at the bottom surface of the block, creating an area of viscous resistance. Because the gap in the self-compensating restrictor may be inaccurate because of manufacturing and assembly errors, an adjustment screw can be used to finely compress or release the two disc springs and thus define the initial gap. This means that the gap in the self-compensating restrictor acts as an area of flow resistance: it can therefore control the rate of oil flow through the gap through the force balance between the oil pressure and stiffness of the disc springs. Oil flowing from the self-compensating restrictor then enters into the single-pad rectangular hydrostatic bearing.

Figure 1(b) illustrates this self-compensating behavior. When a load is applied to the single-pad hydrostatic bearing, the gap in the bearing land  $h_l$  changes to  $h_l + \Delta h_l$  to increase the pocket pressure. As the pocket pressure increases, the gap in the self-compensating restrictor  $h_c$  simultaneously changes to  $h_c + \Delta h_c$ , resulting in higher pocket pressure. In so doing, the variation in the gap in the bearing land is reduced or even eliminated. This indicates that high or infinite stiffness of the hydrostatic bearing is achieved through installation of the proposed self-compensating restrictor.

The lumped parameter modeling model (Bassani, et al., 1992) is adopted herein. This simplifies the hydrostatic bearing as an equivalent electric circuit in accordance with the following considerations:

- The thickness of the fluid film is small, compared with its size in other directions.

- The flow is laminar.
- The body forces are negligible, compared with the viscous forces.
- On the surfaces bounding the fluid film, the velocity of the lubricant matches the velocity of the surfaces.

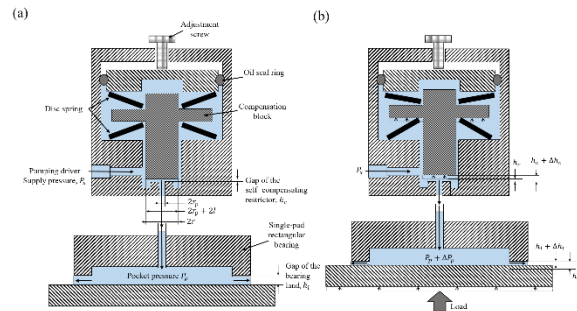


Fig. 1. Cross-sectional view of the hydrostatic bearing system with the proposed self-compensating restrictor: (a) description of parts, (b) force situation.

According to the flow conservation law, the flow that passes through the gap in the self-compensating restrictor is equal to the flow out of the bearing land and can be written as follows:

$$q_c = q_l \tag{1}$$

where  $q_c$  and  $q_l$  denote the flow rates through the gap in the self-compensating restrictor and the bearing land, respectively. Based on the lumped parameter model, Eq. (1) can be rewritten as follows:

$$\frac{P_s - P_p}{R_c} = \frac{P_p}{R_l} \tag{2}$$

where  $R_c$  and  $R_l$  are the flow resistance of the self-compensating restrictor and the bearing land, respectively, and  $P_s$  and  $P_p$  are the supply and pocket pressure, respectively.

The structure of the self-compensating restrictor and the bearing land is illustrated in Fig. 2. Following Slocum (1992), the flow resistance of the restrictor and the bearing land can be obtained thus:

$$R_c = \frac{6\mu \times \ln\left(\frac{r_p + l}{r_p}\right)}{\pi \times h_c^3} = \frac{\gamma_c}{h_c^3} \tag{3}$$

$$R_l = \frac{1}{\frac{\pi \times h_l^3}{6\mu \times \ln\left(\frac{l+w}{r_l}\right)} + \frac{(a+b-4(w+rp)) \cdot h_l^3}{6 \cdot \mu \cdot w}} = \frac{\gamma_l}{h_l^3} \tag{4}$$

where  $\gamma_l$  and  $\gamma_c$  are the structural parameters of the bearing land and the self-compensating restrictor, respectively, and  $h_l$  and  $h_c$  indicate the gaps in the bearing land and the self-compensating restrictor, respectively, and  $\mu$  is the viscosity of oil.

The two flow structural parameters shown in Fig. 2 are related to the shape and size of the bearing structure. The ratio of the flow resistance of the self-compensating restrictor to the bearing land can be derived from Eq. (5).

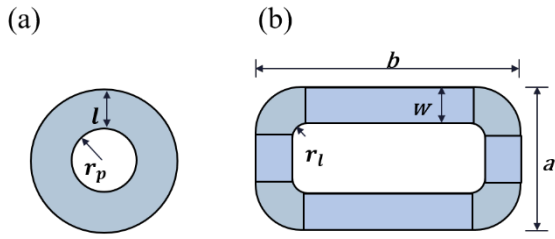


Fig. 2 Schematics of (a) the bottom surface of the self-compensating restrictor and (b) the bearing land.

$$\frac{R_c}{R_l} = \frac{\gamma_c h_l^3}{\gamma_l h_c^3} = C \left( \frac{h_l}{h_c} \right)^3 \quad (5)$$

where  $C$ , the configuration parameter, is relative to the shape and size of the bearing structure. The pocket pressure  $P_p$  can then be written as follows:

$$P_p = \frac{P_s}{1 + C \left( \frac{h_l}{h_c} \right)^3} \quad (6)$$

The bearing load  $W$ , which is also the load-carrying capacity, is expressed as the pocket pressure  $P_p$  multiplied by the effective area of the loading pad  $A_e$ , as shown in Eqs. (7) and (8)

$$W = P_p A_e = \frac{P_s A_e}{1 + C \left( \frac{h_l}{h_c} \right)^3} \quad (7)$$

$$A_e = ab - aw \left( 1 + \frac{b}{a} \right) - 4r_l(r_l + w) + \frac{\pi[(r_l + w)^2 - r_l^2]}{2 \ln(1 + w/r_l)} \quad (8)$$

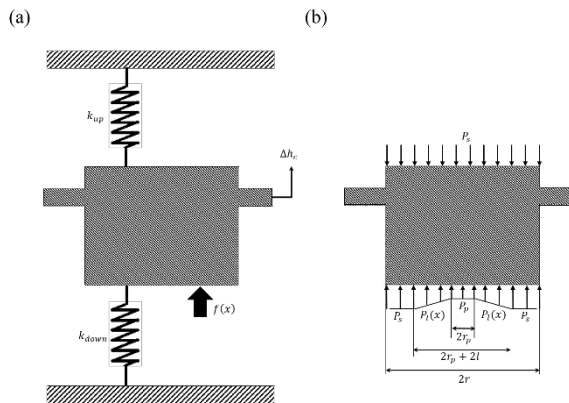


Fig. 3 Free-body diagrams of the compensation block.

To calculate the bearing load  $W$ , the gap in the self-compensating restrictor must first be determined. Figure 3(a) presents a free-body diagram of the compensation block where the spring force and resultant forces are applied to the upper and lower sides of the compensation block. The force balance can be obtained thus:

$$k_{up} \Delta h_c = f(x) + k_{down} \Delta h_c \quad (9)$$

where  $f(x)$  are the forces applied to the top and

bottom surfaces of the compensation block, and  $k_{up}$  and  $k_{down}$  denote the stiffness of the two disc springs. The pressure distribution on the top and bottom surfaces of the compensation block is shown in Fig. 3(b). Due to the bottom surface of the compensating restrictor is flange, the compensation block is displaced by the pressure  $P_s - P_p$  in the region  $0 \leq x \leq r_p$  and the pressure  $P_s - P_i(x)$  in the region  $r_p \leq x \leq r_p + l$ . For the region  $r_p + l \leq x \leq r$ , the pressure is balanced. The resultant force  $f(x)$  of the compensation block displaced by the pocket pressure is given by the following expressions as functions of the radial coordinate  $x$ .

For the region  $0 \leq x \leq r_p$

$$f(x) = (P_s - P_p) \times \int_0^{r_p} 2\pi x dx = (P_s - P_p) \times \frac{\pi r_p^2}{4} \quad (10)$$

For the region  $r_p \leq x \leq r_p + l$

$$f(x) = \frac{2\pi(P_s - P_p)}{\ln\left(\frac{r_p + l}{r_p}\right)} \int_{r_p}^{r_p + l} \ln\left(\frac{x}{r_p + l}\right) [x dx] + 2\pi P_s \int_{r_p}^{r_p + l} x dx$$

$$= \pi(P_s - P_p) \times \left[ \frac{(2r_p l + l^2)}{2 \ln\left(\frac{r_p + l}{r_p}\right)} - r_p^2 \right] + \pi P_s \times (2r_p l + l^2) \quad (11)$$

For the region  $r_p + l \leq x \leq r$

$$f(x) = 0 \quad (12)$$

The gap in the self-compensating restrictor can therefore be written as follows:

$$h_c = h_{c0} + \frac{P_s - P_p}{K_c} \quad (13)$$

$$K_c = \frac{f(x)}{k_{up} + k_{down}} \quad (14)$$

where  $h_{c0}$  is the initial gap in the self-compensating restrictor, and  $K_c$  is the effective rigidity of the compensation block. Eq. (13) expresses the relationship between the gap in the self-compensating restrictor  $h_c$  and the pocket pressure  $P_p$  in the initial design condition. Substituting Eq. (13) into (6) yields the following:

$$P_p = \frac{h_c^3 P_s}{h_c^3 + C h_l^3} = \frac{\left( h_{c0} + \frac{P_s - P_p}{K_c} \right)^3}{\left( h_{c0} + \frac{P_s - P_p}{K_c} \right)^3 + C h_l^3} P_s \quad (15)$$

Because all structural parameters are known, the relationship between the pocket pressure  $P_p$  and the bearing gap  $h_l$  can then be determined. Again, substituting Eq. (15) into (5) yields the following:

$$h_l = \sqrt[3]{\left( \frac{P_s - P_p}{P_p} \right) \cdot \frac{1}{C} \cdot \left[ \frac{\left( h_{c0} + \frac{P_s - P_p}{K_c} \right)^3}{P_p} \right]} \quad (16)$$

Eq. (16) is then differentiated to obtain the stiffness function of the bearing system:

$$K = -A_e \frac{dP_p}{dh_l} = \frac{-3A_{el}K_c P_s h_c^3 - Ch_l^2}{3P_s h_c^2 Ch_l^3 - K_c (h_c^3 + Ch_l^3)^2} \quad (17)$$

The reference gap in the bearing land  $h_{l0}$  was the gap in the bearing land at the dimensionless load  $W/A_e P_s = 0.5$ .

### EXPERIMENTAL SETUP

Figure 4 presents a schematic and corresponding photo of the experimental setup, which was constructed to explore the performance of a single-pad hydrostatic bearing equipped with the proposed self-compensating restrictor. The experimental linear stage consisted of a single-pad bearing in the vertical direction and an opposed-pad bearing in the horizontal direction. The single-pad bearing was the target of the experimental study, and the opposed-pad bearing was employed to constrain the horizontal motion degree of freedom of the bearing. A power screw connected to a load cell was used to apply a vertical load to the single-pad hydrostatic bearing. The gap (i.e., oil-film thickness) of the bearing land therefore changed in accordance with the applied load. Based on the theoretical relationship derived previously, the load, oil-film thickness, pocket pressure, and flow rate were then measured to estimate the load capacity and stiffness of the bearing. The accuracy of the governing equation was then assessed by comparing the experimental results with the theoretical derivation.

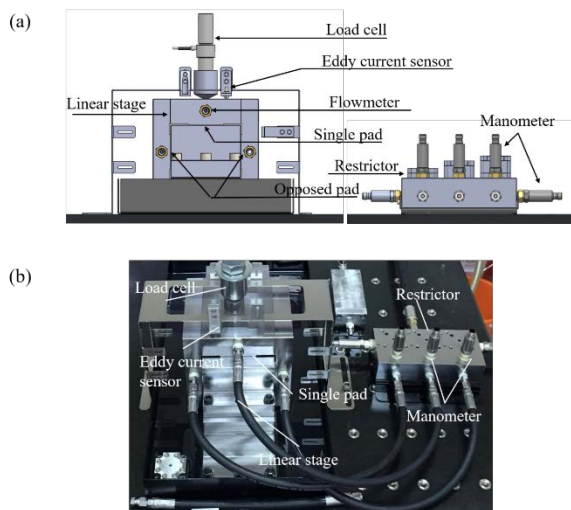


Fig. 4 (a) Schematic and (b) photo of the experimental setup.

### RESULTS AND DISCUSSION

The principal dimensions of the self-compensating restrictor and hydrostatic bearing used for the theoretical derivation and experimental tests are listed in Table 1. Figure 5 shows the effect of supply pressure on the gap in the bearing land and bearing stiffness. Figure 5(a) clearly illustrates that the

curves representing the gap in the bearing land tend to be flat from 0.3 to 0.7 as the oil supply pressure elevates. The gap in the bearing land for  $P_s = 40 \text{ bar}$  remains almost constant as the dimensionless load changes from 0.3 to 0.7. Figure 5(b) shows that the bearing stiffness grows as the supply pressure increases. The highest static stiffness was obtained at  $P_s = 40 \text{ bar}$ , which verifies that the hydrostatic bearing exhibits superior performance when using the proposed self-compensating restrictor.

Table 1: Principal dimensions of the self-compensating restrictor and hydrostatic bearing

Parameter	Value	Parameter	Value
$r_p$	2.5 mm	$b$	150 mm
$l$	1 mm	$h_{c0}$	0.09 mm
$r_l$	7.5 mm	$k_{up}$	1450 N/mm
$w$	15 mm	$k_{down}$	1450 N/mm
$a$	60 mm		

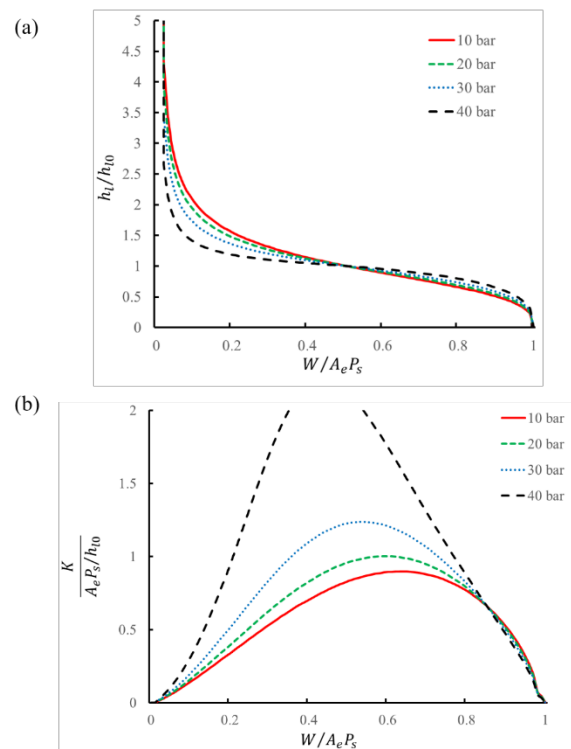


Fig. 5 Effects of supply pressure on (a) the dimensionless gap in the bearing land and (b) the dimensionless stiffness of bearing.

Figure 6 illustrates the effects of supply pressure on the flow resistance of the self-compensating restrictor and the bearing land. Figure 6(a) indicates that the flow resistance of the self-compensating

restrictor varies in accordance with the change in load applied on the bearing. The change in flow resistance of the self-compensating restrictor is most apparent at  $P_s = 40 \text{ bar}$ , which represents the largest displacement of the gap in the self-compensating restrictor. Corresponding with the variation in the resistance of the self-compensating restrictor, Figure 6(b) shows that the bearing land has the largest flow resistance and tends to be constant in the dimensionless load range of 0.3 to 0.7, which implies infinite stiffness of the bearing.

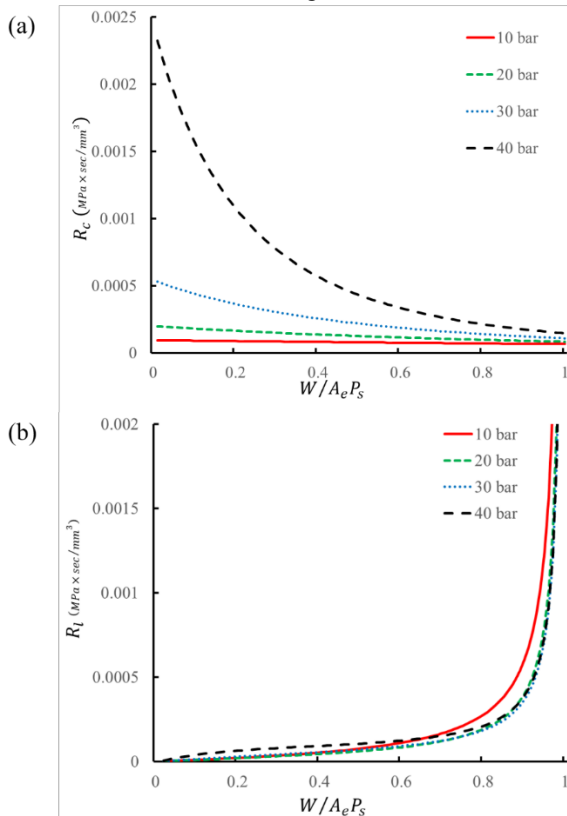


Fig. 6 Effects of supply pressure on (a) the flow resistance of the self-compensating restrictor and (b) the flow resistance of the bearing land.

Figure 7 illustrates the effects of the initial gap in the self-compensating restrictor on the dimensionless gap of the bearing land and dimensionless bearing stiffness at supply pressure  $P_s = 40 \text{ bar}$ . When the initial gap in the self-compensating restrictor is made larger using the adjustment screw, the effect of the self-compensating restrictor becomes less obvious. Eq. (16) represents that, under the same conditions, the gap in the self-compensating restrictor changes by the same amount. In Fig. 7(a), as the initial gap of the self-compensating restrictor is set to  $80 \mu\text{m}$ , the dimensionless gap in the bearing land exhibits minimal change as the dimensionless load varies from 0.3 to 0.7. When the initial gap in the self-compensating restrictor is set to  $70 \mu\text{m}$ , the increase in load from 0.1 to 0.6 appears to

result in an increase in the dimensionless gap of the bearing land, a phenomenon known as negative stiffness. This can cause instability in the bearing system, which is evident in Fig. 7(b).

Figure 8 illustrates the effects of the effective stiffness of the two disc springs on the dimensionless gap in the bearing land and dimensionless bearing stiffness at  $P_s = 40 \text{ bar}$ , where the effective stiffness of the two disc springs is  $k_{up} + k_{down}$ . Figure 8(a) shows that, as the effective stiffness of the two disc springs increases, the compensating ability of the self-compensating restrictor is reduced. Thus, when the effective stiffness of the two disc springs is  $2500 \text{ N/mm}$ , almost no change occurs in the dimensionless gap in the bearing land. This means the bearing system exhibits the best stiffness, as shown in Fig. 8(b). As evident in Fig. 7 and Fig. 8, it is therefore necessary to optimize the initial gap in the self-compensating restrictor as well as the effective stiffness of two disc springs to achieve the best bearing stiffness.

Figure 9 shows adequate consistency between the theoretical analysis and experimental results regarding the dimensionless relationship between the gap of the bearing land and bearing load for  $P_s = 40 \text{ bar}$ . The bearing system in this paper is a single pad hydrostatic bearing system. In the absence of a sufficient preload, the gap in the bearing land will be excessively large, resulting in the fluid failing to meet the theoretical simplification assumptions (Slocum, 1992). Therefore, a large difference exists between the theoretical and experimental results when the dimensionless load is lowered from 0.3 to 0. Another main source of error is attributable to geometric inaccuracies of the restrictor and bearing.

## CONCLUSIONS

This paper proposed a design for a self-compensating flow restrictor for hydrostatic bearings. A lumped parameter modeling method was used to derive an equation describing the relationship between the pocket pressure and resistance provided by both the flow restrictor and the gap in the bearing land. Equations governing the stiffness and load-carrying capacity of the bearing were also derived. The theoretical analysis showed that the bearing system exhibited considerable stiffness because of the parameters of the self-compensating restrictor being properly designed. First, an initial gap in the self-compensating restrictor can be easily corrected using the adjustment screw. Second, the effective stiffness of the two disc springs can be changed using the different stiffness of springs. In this paper, the bearing system exhibited the best stiffness when the initial gap in the self-compensating restrictor was  $70 \mu\text{m}$ , the effective stiffness of the two disc springs was  $2500 \text{ N/mm}$ , and the supply pressure was  $40 \text{ bar}$ . Poorly designed parameters may cause the bearing to display negative

stiffness.

The theoretical derivation was then compared with the experimental results. The influences of the design parameters on bearing stiffness and the feasibility of the new design were demonstrated both analytically and experimentally, although some shortcomings remained. For instance, when the preload was insufficient, a considerable discrepancy was observed between the theoretical analysis and the experimental results. Furthermore, the bearing system continued to exhibit geometric errors. Nevertheless, the theoretical analysis and experimental results were generally consistent in terms of the scope of use (the dimensionless load varies from 0.3 to 0.7). Superior performance with regard to stiffness and the load-carrying capacity to fixed-type restrictors such as the capillary and orifice was achieved. Furthermore, the proposed restrictor possesses the advantage of simplicity with regard to both manufacture and assembly in comparison with membrane-type restrictors.

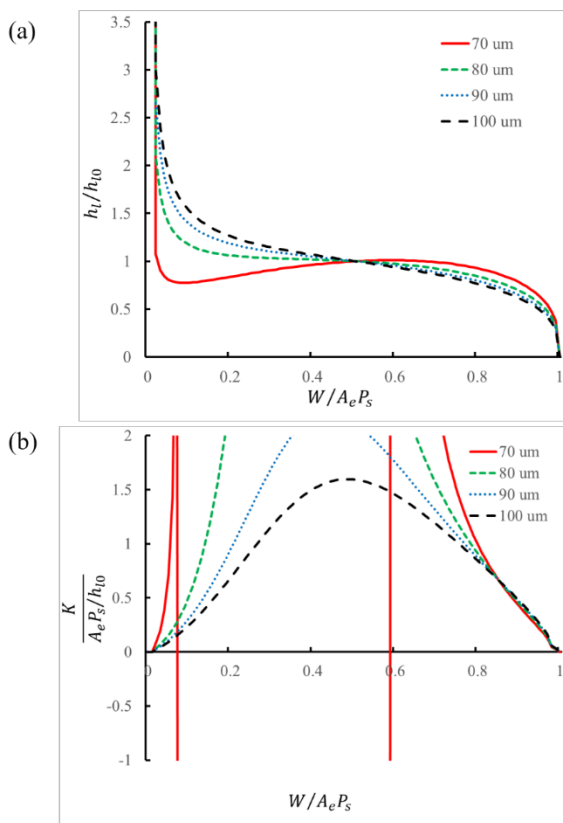


Fig. 7 Effects of the initial gap in the self-compensating restrictor on (a) the dimensionless gap in the bearing land and (b) the dimensionless stiffness of bearing.

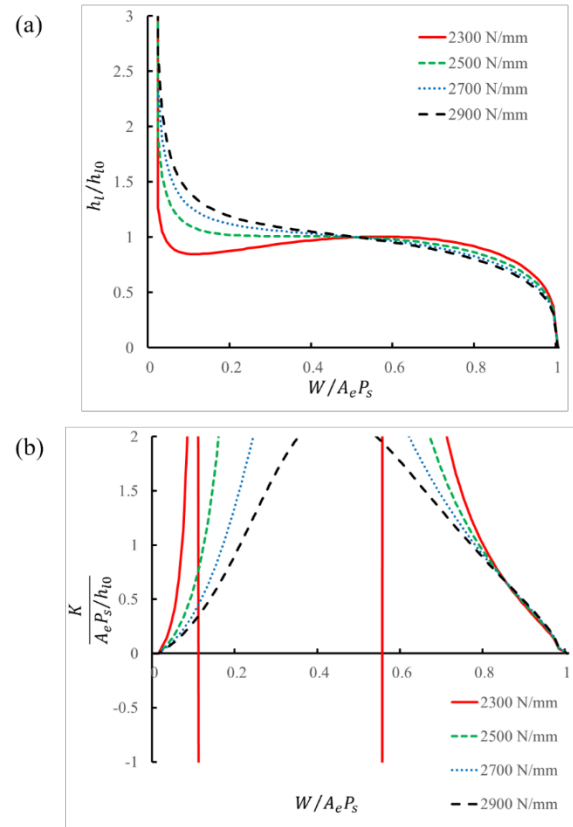


Fig. 8 Effects of the effective stiffness of two disc springs on (a) the dimensionless gap in the bearing land and (b) the dimensionless stiffness of bearing.

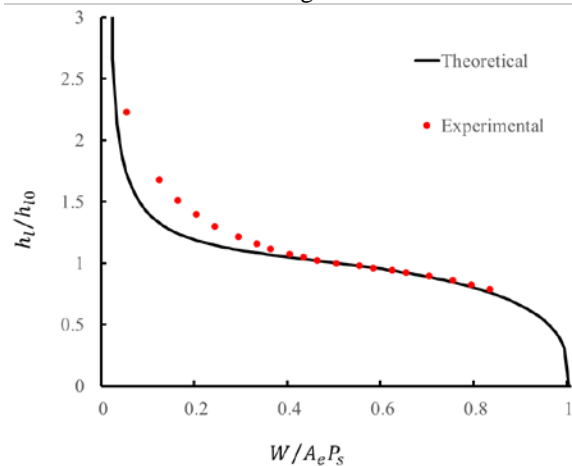


Fig. 9. Comparison of theoretical analysis and experimental results on the dimensionless relationship between the gap in the bearing land and bearing load.

## REFERENCES

Girard, L. D.,” Application des Surfaces Glissantes,”;

- Bachelier, Paris (1862).
- Raimondi, A.A., and Boyd, J., “An analysis of orifice and capillary compensated hydrostatic journal bearing,”; *Lubric. Eng.*, vol. 13, pp. 28-37 (1957).
- Mayer, J. E., and Shaw, M. C., “Characteristics of externally pressurized bearing having variable external flow restrictors,”; *J. Basic Eng.*, vol. 85, pp. 291-296 (1963).
- Mohsin, M. E., “The use of controlled restrictors for compensating hydrostatic bearing,”; *Advances in Mach. Tool Des. and Res.*, pp.429-442 (1962).
- Tully, N., “Static and dynamic performance of an infinite stiffness hydrostatic thrust bearing,”; *J. of Lubrication Tech.*, vol. 99, pp. 106-112 (1977).
- Phalle, V. M., Sharma, S. C., and Jain, S. C., “Influence of wear on the performance of a 2-lobe multirecess hybrid journal bearing system compensated with membrane restrictor,”; *Tribol. Int.*, vol. 44, pp. 380-395 (2011).
- Kotilainen, M. S., “Design and manufacturing of modular self-compensating hydrostatic journal bearings,”; Ph. D. Thesis, Department. of Mechanical Engineering, Massachusetts Institute of Technology, USA (2000).
- Kang, Y., Shen, P. C., Chang, Y. P., Lee, H. H., and Chiang, C. P., “Modified predictions of restriction coefficient and flow resistance for membrane-type restrictors in hydrostatic bearing by using regression,”; *Tribol. Int.*, vol. 40, pp. 1369-1380 (2007).
- Lai, T. H., Chang, T. Y., Yang, Y. L., and Lin, S. C., “Parameters design of a membrane-type restrictor with single-pad hydrostatic bearing to achieve high static stiffness,”; *Tribol. Int.*, vol. 107, pp. 206-212 (2017).
- Gohara, M., Somaya, K., Miyatake, M., and Yoshimoto, S., “Static characteristics of a water-lubricated hydrostatic thrust bearing using a membrane restrictor,”; *Tribol. Int.*, vol. 75, pp. 111-116 (2014).
- Bassani, R., and Piccigallo, B., “Hydrostatic lubrication,” Elsevier Science, Nederland (1992).
- Slocum, A. H., “Precision Machine Design,”; Society of Manufacturing Engineers, Michigan, USA (1992).
- $f(x)$  : the forces applied to the top and bottom surfaces of the compensation block
- $h_c$  : the gap in the self-compensating restrictor
- $h_{c0}$  : the initial gap in the self-compensating restrictor
- $h_l$  : the gap in the bearing land
- $h_{l0}$  : the reference gap in the bearing land
- $K_c$  : the effective rigidity of the compensation block
- $k_{down}$  : the stiffness of the bottom disc spring
- $k_{up}$  : the stiffness of the top disc spring
- $l$  : the thickness of the gap in the self-compensating restrictor
- $P_p$  : the pocket pressure
- $P_s$  : the supply pressure
- $q_c$  : the flow rate through the gap in the self-compensating restrictor
- $q_l$  : the flow rate through the bearing land
- $R_c$  : the flow resistance of the self-compensating restrictor
- $R_l$  : the flow resistance of the bearing land
- $\gamma_c$  : the structural parameters of the self-compensating restrictor
- $\gamma_l$  : the structural parameters of the bearing land
- $r_l$  : the inner radius of the bearing land
- $r_p$  : the inner radius of the gap in the self-compensating restrictor
- $\mu$  : the viscosity of oil
- $w$  : the thickness of the bearing land
- $W$  : the load of the bearing

## NOMENCLATURE

- $a$  : the width of the bearing land
- $A_e$  : the effective area of the loading pad
- $b$  : the length of the bearing land
- $C$  : the configuration parameter

# 液靜壓軸承自補償截流器 之新穎設計

楊倬昱 高惟禎 王翊承 宋震國  
國立清華大學動力機械工程學系

## 摘要

本文設計了一種用於液靜壓軸承的自補償節流器。自補償節流器主要由一個補償塊和兩個盤形彈簧組成，具有自補償和易於安裝的特點。首先本文建立了理論模型。接著通過理論和實驗比較了不同的設計參數對軸承性能的影響以及新設計的可行性。將理論分析的結果與實驗的結果進行比較。在剛性和承載能力方面獲得了優異的性能。